Lorentz-Lorenz coefficient, critical point constants, and coexistence curve of 1,1-difluoroethylene

Nicola Fameli* and David A. Balzarini
Department of Physics and Astronomy, The University of British Columbia, 6224 Agricultural Road, Vancouver, B.C., Canada V6T 1Z1
(Received 14 May 2005; published 7 November 2005; publisher error corrected 10 November 2005)

We report measurements of the Lorentz-Lorenz coefficient density dependence $\mathcal{L}(\rho)$, the critical temperature T_C, and the critical density ρ_C of the fluid 1,1-difluoroethylene ($H_2C_2F_2$). Lorentz-Lorenz coefficient data were obtained by measuring refractive index n, and density ρ of the same fluid sample independently of one another. Accurate determination of the Lorentz-Lorenz coefficient is necessary for the transformation of refractive index data into density data from optics-based experiments on critical phenomena of fluid systems done with different apparatuses, with which independent measurement of n and ρ is not possible. Measurements were made along the coexistence curve of the fluid and span the density range 0.01 to 0.80 g cm^{-3}. The Lorentz-Lorenz coefficient results show a stronger density dependence along the coexistence curve than previously observed in other fluids, with a monotonic decrease from a density of about 0.2 g cm^{-3} onward, and an overall variation of about 2.5% in the density range studied. No anomaly in the Lorentz-Lorenz function was observed near the critical density. The critical temperature is measured at $T_C=(302.964\pm0.002)$ K (29.814 °C) and the measured critical density is $\rho_C=(0.4195\pm0.0018)$ g cm^{-3}.

DOI: 10.1103/PhysRevE.72.056105 PACS number(s): 64.60.Fr

I. INTRODUCTION

We have accurately measured the density dependence of the Lorentz-Lorenz coefficient of 1,1-difluoroethylene ($H_2C_2F_2$), its critical temperature, and critical density. The experiments presented herein constitute a preparatory phase to a set of other experiments we are carrying out with a different apparatus from the one described in this article. The latter set of experiments will combine three different optical techniques in one apparatus for the study of critical phenomena in pure fluids [1,2], as well as the mapping of the *P-V-T* space of a fluid. Said optical techniques produce measurements of the index of refraction of the fluid under study. However, to be able to interpret experimental results on critical phenomena in fluids obtained through this apparatus and to compare them with theoretical predictions, the refractive index data have to be transformed into density data, as density is the quantity typically used by theories in their description of this class of critical phenomena (for example, for the order parameter describing the coexistence curve temperature dependence) [3]. As a result, we need to measure the Lorentz-Lorenz coefficient, which is the purpose of the experiments described below.

The substance investigated in the reported experiments was chosen for its relatively easily accessible critical point, the limited amount of accurate data on its critical region, and its Lorentz-Lorenz coefficient available in the literature. In general, we have noticed a scarcity of the Lorentz-Lorenz coefficient and critical point data on hydrocarbons.

The Lorentz-Lorenz coefficient $\mathcal{L}$ relates the index of refraction n to the density of a gas, ρ, in the following way:

$$\frac{n^2-1}{n^2+2}=\rho\mathcal{L}(n,\rho). \tag{1}$$

This relation is the optical frequency equivalent of the Clausius-Mossotti relation for the dielectric constant, at lower frequencies of the electromagnetic spectrum [4,5]. Equation (1) is used in obtaining experimental data on fluid density from the measurements of the refractive index ([6–9]).

One can relate the refractive index to density using a *P-V-T* curve, for example, by measuring the refractive index as a function of pressure and then relying on an equation of state to relate pressures to densities. However, it is clearly more desirable not to rely on any previous data to relate the refractive index and the density of the sample at hand, since such data are necessarily obtained with different samples, containing, in general, different percentages or types, of impurities. Correlation of results from separate experiments can often lead to inaccurate or incorrect conclusions, especially in experiments where we have diverging quantities and where precise temperature control is necessary, as is the case near the critical point. To avoid this problem, it necessary to have an accurate estimate of the Lorentz-Lorenz coefficient, with the index of refraction and density measured on the same sample, and independently of one another.

We have therefore carried out measurements of the Lorentz-Lorenz coefficient of 1,1-difluoroethylene using a self-contained apparatus, which enables us to measure separately the index of refraction and the density of the fluid in question.

Early investigations of the Lorentz-Lorenz coefficient were carried out on pure fluids and mixtures at low densities, and generally showed a linear increase with density [10]. Some experiments showed an anomaly near the critical density. However, these experiments measured refractive index only and required *P-V-T* data from other experiments for analysis and interpretation [11]. Our measurements of $\mathcal{L}$ show a departure from both of these features.

*Corresponding author. Present address: Department of Anesthesiology, Pharmacology and Therapeutics, The University of British Columbia, 2176, Health Sciences Mall, Vancouver, B. C., Canada V6T 1Z3. Electronic address: fameli@physics.ubc.ca

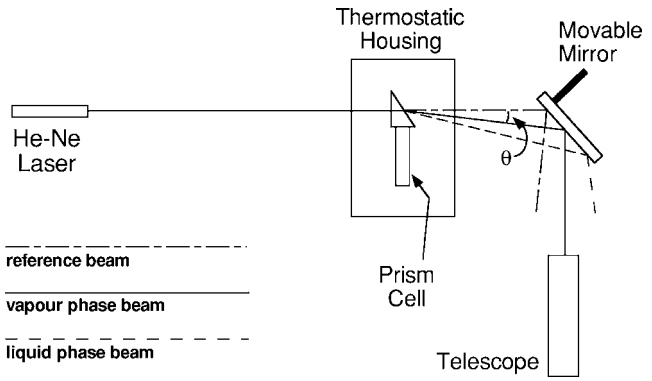

FIG. 1. Schematic diagram of the experimental apparatus (not to scale).

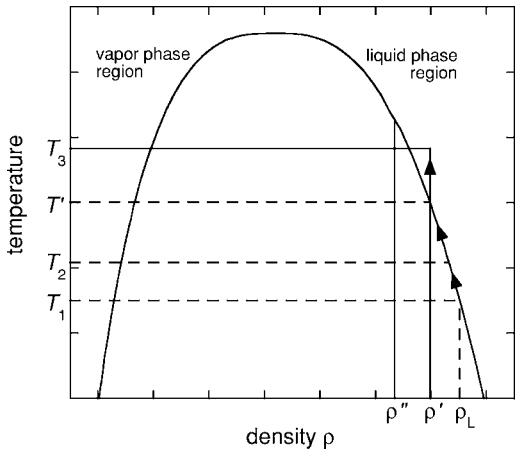

FIG. 2. Qualitative temperature-density phase diagram of the vapor coexistence curve of $H_2C_2F_2$. This graph depicts the steps taken to obtain the Lorentz-Lorenz coefficient. The sample cell is initially filled to a density, ρ', inserted in the thermostat set a temperature $T_1 < T'$ and the liquid phase refractive index, $n_L(\rho', T_1)$, is measured. The temperature is then increased to T_2 and $n_L(\rho', T_2)$ is measured and found to be different from $n_L(\rho', T_1)$ as long as $T_2 < T'$. The procedure is repeated until, for temperatures above T', the measured $n_L(\rho', T)$ is practically independent of temperature. The system is then in the one phase region outside the coexistence curve and measurements of the refractive index in this situation yield $n_L(\rho', T')$, needed for the determination of $\mathcal{L}$ at density ρ'. The sample is then brought to another density ρ'' by bleeding out some fluid and the procedure repeated to obtain $n_L(\rho'', T'')$, and so on.

II. EXPERIMENTAL METHOD

The substance studied, 1,1-difluoroethylene (also known as vinylidene fluoride, molecular weight 64.035 g mol^{-1}), is a colorless, flammable, nontoxic gas at room temperature and atmospheric pressure. Its main use is in preparing polymers and copolymers and as an intermediate in organic synthesis [12]. The material used in these experiments was purchased from Scott Specialty Gases and is of 99.4% purity.

In these experiments, the sample is introduced in a high pressure container (the "prism cell" of Fig. 1), which has a prism-shaped section, about 1 cm in height, formed between two sapphire windows at one end of the cell [13]. Sample temperature is maintained at a chosen value by inserting the sample cell in a thermostat capable of regulating temperature within 0.5 mK. The experimental arrangement is shown schematically in Fig. 1.

The sample cell is filled with fluid at a high density and weighed. It is then placed in the thermostatic housing. We measure the angle of deviation θ with respect to the reference beam, of a laser beam (He-Ne laser, $\lambda = 632.8$ nm) traversing the prism-shaped fluid sample. The beam is expanded to a diameter of about 2.5 cm and collimated to ensure coverage of the entire sample cross section. With this setup, when both liquid and vapor are present in the cell, both phases are sampled at the same time. The deviation angle depends on the refractive index of the fluid. The micrometer screw on the adjustable mirror is calibrated to relate the micrometer scale reading to the refraction angle.

During the measurements, if the temperature is such that the fluid is below the coexistence curve, both liquid and vapor phases are present. Since the region of interest is just outside the coexistence curve, the temperature is gradually increased until no further change is measured in the angle of deviation. This corresponds to having the fluid in a single phase (Fig. 2 summarizes this procedure graphically). The sample cell is then removed from the thermostatic housing and weighed again. This provides one datum of the deviation angle and the sample cell mass. Some fluid is bled from the sample, and the procedure is repeated to provide another measurement. This measurement sequence is repeated until the sample density is close to the critical value. At this stage of the experiment, the coexistence curve is measured by returning the sample to the low temperature end of the measurement sequence and recording the deviation angle of the laser beam in the liquid and vapor phases as a function of sample temperature. Critical temperature and critical density of the sample are then obtained from these data.

Following the coexistence curve determination, measurements of mass and deviation angles are resumed until the sample cell is empty, to complete the data set for the Lorentz-Lorenz coefficient determination from the critical density to near-zero density. This results in a series of measurements of the deviation angle versus sample mass corresponding to the region just above the coexistence curve. The reason for choosing this region in which to measure the Lorentz-Lorenz coefficient, is to be able to use this data in interpreting measurements of the coexistence curve and critical point constants from this and other experiments.

The mass measurements $m_{\text{cell+fluid}}$ are of the sample fluid plus the sample container masses, hence the mass of the fluid alone is obtained by subtracting the mass of the empty cell, m_{cell}, from the measured mass. Then, having measured the volume of the container, V, the sample density ρ_{fluid} is obtained: $\rho_{\text{fluid}} = (m_{\text{cell+fluid}} - m_{\text{cell}})/V$. The volume of the sample container is determined by filling it with distilled water and weighing it. The volume of our experimental cell is (12.066 ± 0.003) cm^3, including a small correction accounting for volume change with temperature.

The index of refraction is obtained by optical analysis. First, the adjustable mirror micrometer screw scale calibration equation is determined. This is obtained by placing a

diffraction grating in the same position that the sample occupies during the measurements and taking readings on the micrometer scale of the diffraction maxima. These are, in turn, related to the refraction angle θ giving a linear relationship between the micrometer scale and the beam deflection angle [2]. After this calibration stage, application of Snell's law to our optical system leads to a measurement of the refractive index of the fluid, n_{fluid}, as a function of the refraction angle, θ. Care must be exercised in this step of the analysis in order to eliminate any effects of possible wedge angles in the windows. Any wedges between the cell window faces were measured at the same time that the internal angle of the hollow prism was measured, and were accounted for in our analysis [14]. The angle of the hollow prism was also measured with high pressure in the cell in order to take into account any significant effects on the experimental measurements. The distortion of the volume of the experimental cell with pressure is negligible in the pressure range of the present experiment (up to about 15 MPa). Measurements of the index of refraction are taken across the whole sample cross section. The accuracy of the refractive index determination near the critical point is limited by the strong density gradient caused by the large compressibility [13–15]. Therefore, near the critical point, the refractive index measurements are taken at a sufficiently high temperature (above T_C) to avoid beam distortion. In our experiments, the sample was heated to temperatures between 0.6 and 0.9 K above the critical temperature to take optical readings for the determination of the Lorentz-Lorenz coefficient close to the critical density. In Ref. [15], a relationship is suggested [Eq. (3.5), Sec. III], that indicates when density gradients effects due to earth's gravitational field can be neglected in a fluid near its critical point. Applying such an equation to 1,1-difluoroethylene reveals that temperatures differences $T-T_C$ of the order of 0.5 K delimit the region, beyond which the density profile near the critical point is no longer strongly influenced by gravity.

III. RESULTS AND DISCUSSION

A. Lorentz-Lorenz coefficient

Results of the Lorentz-Lorenz coefficient measurements, $\mathcal{L}$, versus density are plotted in Fig. 3. The data refer to two separate measurement sequences carried out during an eight-month period, on two samples of 1,1-difluoroethylene extracted from the same lecture bottle. One of the two runs (black circles) extended to a higher density range than the other (dotted circles).

The value of $\mathcal{L}$ varies by approximately 2.5% over the density range studied in this experiment, exhibiting a dependence on the density along the coexistence curve, with a gentle maximum in the neighborhood of $\rho=0.2$ g cm^{-3}. Around the critical density ρ_C where an accurate determination of $\mathcal{L}$ is more crucial for our purposes, the measured value of the Lorentz-Lorenz coefficient varies by less than 1% in both sequences.

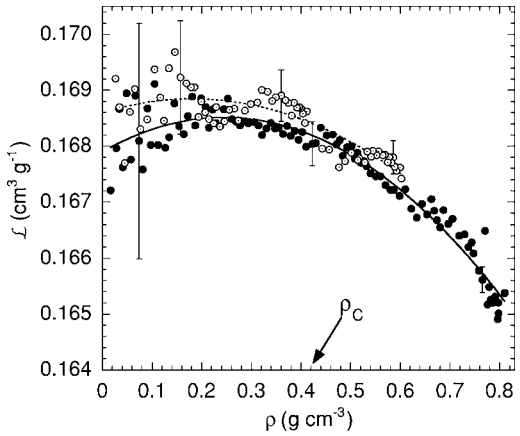

FIG. 3. Measured density dependence of the Lorentz-Lorenz coefficient ($\mathcal{L}$) of 1,1-difluoroethylene. The solid and dotted curves are quadratic fits to the data according to Eq. (2). The fit parameters are in Table I.

The Lorentz-Lorenz coefficient can be expressed in a so-called refractometric virial expansion in powers of the density [13]

$$\mathcal{L}(\rho) = \mathcal{L}_0 + \mathcal{L}_1\rho + \mathcal{L}_2\rho^2 + \ldots \tag{2}$$

The solid and dotted lines shown in the graph of Fig. 3 represent quadratic fits to the two series of data and yield the values of the coefficients $\mathcal{L}_0$, $\mathcal{L}_1$, and $\mathcal{L}_2$ reported in Table I.

Data at the low density end of the range investigated are affected by larger errors than the data around the critical density and larger density regions. At low densities, the accuracy in the determination of $\mathcal{L}$ is mainly limited by how accurately the mass of the empty prism cell can be measured at the end of the experiment. As the quantity one needs is the difference $m_{\text{cell+fluid}}-m_{\text{cell}}$, where m_{cell} is the mass of the empty cell, the same degree of uncertainty in the empty cell mass yields a larger inaccuracy in the determination of $\mathcal{L}$ at the low density than in the higher density measurements. Hence, the larger scatter in the data in the low density region of the measurements.

At the high density end of the data, one must be aware of another experimental pitfall. At those densities the liquid-vapor coexistence curve of 1,1-difluoroethylene is at tem-

TABLE I. Results of a quadratic fit to the Lorentz-Lorenz data of 1,1-difluoroethylene ($C_2H_2F_2$). $\mathcal{L}_C$ is the critical Lorentz-Lorenz coefficient calculated from the critical density ρ_C (see the procedure described in the text.)

	$\mathcal{L}_0$(cm^3 g^{-1})	$\mathcal{L}_1$(cm^6 g^{-2})	$\mathcal{L}_2$(cm^9 g^{-3})	$\mathcal{L}_C$(cm^3 g^{-1})
Run 1 (⊙)	0.169±0.002	0.003±0.003	−0.008±0.004	0.1685±0.0017
Run 2 (•)	0.168±0.002	0.005±0.002	−0.010±0.002	

peratures much lower than the typical room temperature, which was monitored often during the experiment and found to average around 23.3 °C. The reported data were taken starting at high densities, which meant maintaining the cell at temperatures of about +3 °C in the thermostat. Clearly then, when the cell is removed from the thermostatic housing to be weighed, condensation and then evaporation of atmospheric moisture on the cell body occurs quite rapidly thereby hindering accurate measurement of the cell mass. At the same time, at high densities, we could not afford to leave the cell out of the thermostat for very long to wait for the condensation-evaporation effect to equilibrate, since, in so doing, the entire sample would have quickly gone into the liquid phase region of its phase diagram, rapidly reaching high enough pressures to cause possible damage to the experimental cell. Instead, to minimize this risk, a study of the consequences of the moisture condensation-evaporation phenomenon was done at the end of the experiment with the empty cell. It was found that when the difference between the thermostat temperature and room temperature was the highest, the overall effect led to an underestimation of about 0.5% of the value of $\mathcal{L}$ corresponding to the region at densities $\rho > 0.75$ g cm^{-3}. The monotonic decrease in the data in that density range is partially due to this effect.

Within experimental error, the data from the two experimental runs overlap reasonably well and the slight discrepancies between the two sets can be ascribed to differences in the amount of impurities in the samples. Previous studies of the effect of small impurities on measurements of critical point constants have shown that the critical temperature is much more sensitive to impurities than the critical density [14,16].

The estimated uncertainty in the $\mathcal{L}$ measurements is comparable to the scatter of data in the graph, as is illustrated by the error bars in Fig. 3. It is about 2×10^{-4} cm^3 g^{-1} near the critical density. This variation in $\mathcal{L}$ is consistent with measurements made on other fluids in this laboratory [13,14,17]. Moreover, as is apparent from Fig. 3, we do not observe any anomaly in the density dependence of the Lorentz-Lorenz coefficient near the critical point, within the limitations imposed on our optical technique by the strong density gradients occurring in pure fluids close to their critical point. This result is in agreement with earlier theoretical studies on the subject [11,18,19].

From the Lorentz-Lorenz data, we also obtained the electronic (optical) polarizability α_p of 1,1-difluoroethylene using the relationship $\lim_{\rho \to 0} \mathcal{L}(\rho) = (4\pi\alpha_p/3)N_A$, with N_A as Avogadro's number [10]: the result is $\alpha_p = (4.29 \pm 0.04)$ Å^3.

B. Coexistence curve, critical temperature, and critical density

The liquid-vapor coexistence curve of 1,1-difluoroethylene was also measured in this experiment. This was done after the sample had been bled to the point corresponding as closely as possible to the critical density. The refractive index of the two coexisting phases was measured as a function of temperature and then transformed into a set of density measurements by means of the Lorentz-Lorenz coefficient measured as described in Sec. III A. From these data, the critical temperature T_C and the critical density ρ_C can be extracted. The coexistence curve data obtained in our experiments are shown in Fig. 4.

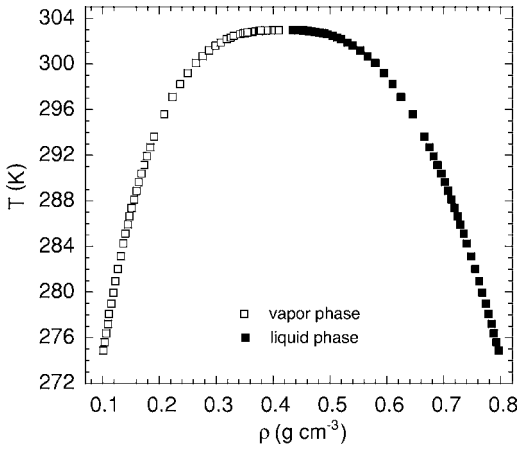

FIG. 4. Coexistence curve data obtained for 1,1-difluoroethylene; white squares correspond to vapor phase, black squares to liquid phase.

The data have been analyzed in terms of renormalization group and scaling theory [3,20,21], and are fitted to an equation of the form

$$\Delta\rho^* \equiv \frac{\rho_L - \rho_V}{2\rho_C} = B_0 t^\beta \left(1 + B_1 t^\Delta + B_2 t^{2\Delta} + \cdots\right), \qquad (3)$$

relating the order parameter $\Delta\rho^*$ to the reduced temperature $t = (1 - T/T_C)$. ρ_C is the critical density, β the order parameter critical exponent, and Δ the correction-to-scaling critical exponent.

Figure 5 is a log-log plot of $\Delta\rho^*/t^\beta$ as a function of the reduced temperature, t, and it represents the coexistence curve data according to Eq. (3). The line interpolating the data is a fit with two correction-to-scaling terms, with $\beta = 0.326$ and $\Delta = 0.50$ held fixed in the fits. The critical ampli-

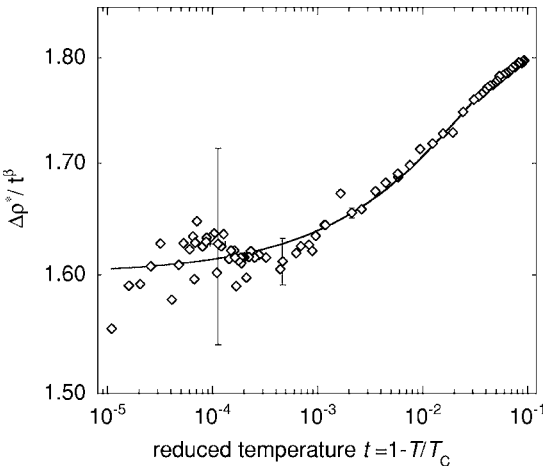

FIG. 5. The log-log plot of the order parameter data of 1,1-difluoroethylene. The line represents data interpolation using Eq. (3) over the range $10^{-5} < t < 10^{-1}$, with $\beta = 0.326$ and $\Delta = 0.50$.

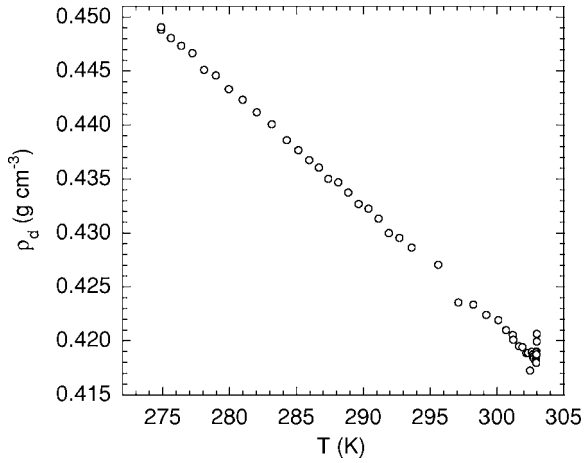

FIG. 6. Coexistence curve diameter data, ρ_d, of 1,1-difluoroethylene.

tude values B_0, B_1, and B_2 obtained are as follows: $B_0 = 1.601 \pm 0.008$, $B_1 = 0.71 \pm 0.06$, $B_2 = -1.10 \pm 0.16$. The temperature range at which the coexistence curve data can be obtained is limited as the critical point is approached because of "gravitational rounding" resulting from the increasing compressibility, as mentioned at the end of Sec. II. In the reported measurements the coexistence curve of $C_2H_2F_2$ was measured over the reduced temperature interval $10^{-5} < t < 10^{-1}$. However, the pronounced density gradients in the fluid nearing its critical region render it arduous to take accurate data at values of $t \lesssim 10^{-4}$, as the much larger scatter in the data at low values of t in Fig. 5 shows.

In spite of this, we can still obtain an accurate estimate of the critical density ρ_C from the measured coexistence curve data by the following procedure. First, the critical temperature T_C is obtained by fitting the coexistence curve data to a power law of the same form as Eq. (3), but expressed in terms of the density difference $\Delta\rho$ alone, not divided by the critical density, as the latter is yet to be determined at this stage. Secondly, from the fluid's coexistence curve expressed in terms of the refractive index data, n_L and n_V, the critical refractive index n_C is calculated from the coexistence curve diameter $n_d \equiv (n_L + n_V)/2$. As $T \to T_C$, $n_d \to n_C$, in accordance with the "law of rectilinear diameter," which has been verified to hold for pure fluids [22], and it is also well obeyed by 1,1-difluoroethylene, as the data in Fig. 6 illustrate. The larger scatter in the data near the critical temperature is due to loss of accuracy in the measurements caused by high density gradients close to the critical point. This value of n_C is then used in a plot of the Lorentz-Lorenz coefficient, $\mathcal{L}$ vs n, to yield the critical value of $\mathcal{L}_C = \mathcal{L}(n_C)$. Lastly, the values of n_C and $\mathcal{L}_C$, and Eq. (1) give the critical density, $\rho_C = (1/\mathcal{L}_C)(n_C^2 - 1)/(n_C^2 + 2)$.

To have a reliable value of the critical temperature, two correction-to-scaling terms must be retained in Eq. (3), while the critical temperature is treated as a free parameter in a nonlinear least-squares fit of the data. In this experiment, we obtained a value of $T_C = (302.964 \pm 0.002)$ K for the critical temperature of 1,1-difluoroethylene. The measured values for the critical refractive index and critical Lorentz-Lorenz coefficient are: $n_C = 1.1082 \pm 0.0006$ and $\mathcal{L}_C = (0.1685 \pm 0.0017)$ cm^3 g^{-1}, respectively. We measured the critical density of 1,1-difluoroethylene as $\rho_C = (0.4195 \pm 0.0018)$ g cm^{-3}.

TABLE II. Critical temperature and density of 1,1-difluoroethylene ($C_2H_2F_2$).

Source	T_C(K)	ρ_C(g cm^{-3})
Ref. [26]	303.25±0.50	0.417±0.010
Ref. [27]	302.74±0.005	0.41±0.02
Ref. [25]	302.9	0.42
This article	302.964±0.002	0.4195±0.0018

The coexistence curve results shown in Fig. 5 display the typical trend of pure fluid, namely that the coefficient B_1 for the first correction-to-scaling term of Eq. (3) is positive, as noticeable in the graph for $t > 7 \times 10^{-4}$.

In one of our Lorentz-Lorenz coefficient data sets (black circles in Fig. 3), we observed a slight increase at low densities up to a value of $\rho \simeq 0.2$ g cm^{-3}, where $\mathcal{L}$ has a maximum. The other set of data (dotted circles in Fig. 3) is relatively constant in the same range. Both sets display a more marked monotonic decrease than previously observed in other fluids in the rest of density interval explored ($0.2 < \rho < 0.8$) g cm^{-3}. We find no indication of singular behavior in the vicinity of the critical density. These features of the Lorentz-Lorenz coefficient of 1,1-difluoroethylene are, to a certain extent, a departure from similar measurements on other fluids. Previously, the Lorentz-Lorenz data either had a maximum at the critical density [17,23] or did not display any strong monotonic trend [10]. Other measurements showed a maximum for $\mathcal{L}(\rho)$ at a density below the critical density, but no strong monotonic decrease at higher densities [16].

Some experimenters have measured deviations from the Lorentz-Lorenz relation. For example, Beysens *et al.* measured discrepancies in the refractive index temperature coefficient at constant pressure $(\partial n/\partial T)_P$ [24]. Others have indirectly determined values of the Lorentz-Lorenz coefficient using their own refractive index measurements and tabulated values of density at known points, but their evaluations of the coefficient were carried out at only one point for each substance and are, therefore, of limited use in the search for any trends in the variation of the Lorentz-Lorenz coefficient with density [6,7].

We report in Table II a list of critical temperature and critical density measurements for 1,1-difluoroethylene found in the literature. Our data agree well with these previously available results on the critical density and provide an improvement upon them. The slightly more marked discrepancies between our determination of the critical temperature and that found in these publications is likely due to different amounts and types of impurities in the samples [18]. We have been unable to find any published material on the Lorentz-Lorenz coefficient of research grade 1,1-difluoroethylene. Our experiments have therefore yielded accurate measurements of the Lorentz-Lorenz coefficient of this material over a wide range of densities.

ACKNOWLEDGMENTS

We wish to thank Sharlene Tennant for her contribution to the conduction of the experiments. N.F. is also grateful to Douw Steyn for helpful input in the manuscript and to Luisa Canuto for help in the data taking process. This research was supported in part by grants from the National Sciences and Engineering Research Council of Canada to D.A.B.

[1] K. T. Pang, Ph. D. thesis, The University of British Columbia, Vancouver, B. C., Canada, 1994 (unpublished).
[2] N. Fameli, Ph. D. thesis, The University of British Columbia, Vancouver, B. C., Canada, 2000, Sect. 5.4 (unpublished).
[3] M. E. Fisher, in *Scaling, Universality and Renormalization Group Theory*, Lecture Notes in Physics, Vol. 186, edited by F. J. W. Hahne (Springer, Berlin, 1982), pp. 1–139.
[4] M. Born and E. Wolf, *Principles of Optics* (Pergamon Press, London, 1959), Sect. 2.3.3.
[5] J. D. Jackson, *Classical Electrodynamics*, 2nd ed. (John Wiley and Sons, New York, 1975), Sect. 4.5.
[6] H. B. Chae, J. W. Schmidt, and M. R. Moldover, J. Phys. Chem. **94**, 8840 (1990).
[7] J. W. Schmidt and M. R. Moldover, J. Chem. Eng. Data **39**, 39 (1994).
[8] J. Yata, M. Hori, M. Niki, Y. Isono, and Y. Yanagitani, Fluid Phase Equilib. **174**, 221 (2000).
[9] A. Oleinikova and H. Weingärtner, Chem. Phys. Lett. **319**, 119 (2000).
[10] A. D. Buckingham and C. Graham, Proc. R. Soc. London **A337**, 275 (1974).
[11] J. M. Lucas and B. L. Smith, Phys. Lett. **19**, 22 (1965).
[12] W. Braker and A. L. Mossman, *Matheson Gas Data Book*, 6th ed (Matheson, Lyndhurst, NJ, 1980), pp. 476–480.
[13] D. Balzarini and P. Palffy, Can. J. Phys. **52**, 2007 (1974).
[14] U. Närger and D. A. Balzarini, Phys. Rev. B **42**, 6651 (1990).
[15] M. R. Moldover, J. V. Sengers, R. W. Gammon, and R. J. Hocken, Rev. Mod. Phys. **51**, 79 (1979).
[16] J. R. Hastings, J. M. H. Levelt Sengers, and F. W. Balfour, J. Chem. Thermodyn. **12**, 1009 (1980).
[17] M. Burton and D. Balzarini, Can. J. Phys. **52**, 2011 (1974).
[18] J. V. Sengers, D. Bedeaux, P. Mazur, and S. C. Greer, Physica A **104**, 573 (1980).
[19] S. Y. Larsen, R. D. Mountain, and R. Zwanzig, J. Chem. Phys. **42**, 2187 (1965).
[20] K. G. Wilson, Phys. Rev. B **4**, 3174 (1971); **4**, 3184 (1971).
[21] F. J. Wegner, Phys. Rev. B **5**, 4529 (1972).
[22] L. Caitellet and E. C. Matthias, C. R. Hebd. Seances Acad. Sci. (Paris) **102**, 1202 (1886).
[23] P. Palffy-Muhoray and D. Balzarini, Can. J. Phys. **56**, 1140 (1978).
[24] D. Beysens and P. Calmettes, J. Chem. Phys. **66**, 766 (1977).
[25] *CRC Handbook of Chemistry and Physics*, 85th ed., edited by David R. Lide (CRC Press, Boca Raton, FL 2005.)
[26] W. H. Mears, R. F. Stahl, S. R. Orfeo, R. C. Shair, L. F. Kells, W. Thompson, and H. McCann, Ind. Eng. Chem. **47**, 1449 (1955).
[27] D. S. Tsiklis and V. M. Prokhorov, Russ. J. Phys. Chem. **41**, 1182 (1967).